ELSEVIER

Physics of the Earth and Planetary Interiors 107 (1998) 233–248

PHYSICS OF THE EARTH AND PLANETARY INTERIORS

Geochemical characteristics of the uppermost mantle beneath the Japan island arcs: implications for upper mantle evolution

Natsue Abe [a,*], Shoji Arai [a], Hisayoshi Yurimoto [b]

[a] *Department of Earth Sciences, Kanazawa University, Kanazawa 920-11, Japan*
[b] *Department of Earth and Planetary Sciences, Tokyo Institute of Technology, Tokyo 152, Japan*

Received 15 August 1995; revised 20 June 1996; accepted 15 September 1996

Abstract

Geochemical characteristics of clinopyroxene in peridotite xenoliths from three volcanos, Megata, On-yama and Kurose, in the Japan arcs are important for understanding igneous and metasomatic processes within the mantle wedge. The clinopyroxenes in peridotite xenoliths from the Japan arcs are clearly different from those in abyssal peridotites and the peridotite xenoliths from other tectonic settings, such as continental rifts and oceanic hotspots. Geochemical characteristics of the sub-arc clinopyroxenes are not apparently related either to degree of hydration or to degree of refractoriness, but are consistent from one sample to another. The REE patterns vary from LREE-depleted pattern to flat or slightly LREE-enriched patterns. Then their $(Ce/Yb)_N$ (subscript N = chondrite-normalized) vary widely from 0.04 to 4.0. On the other hand the Ti/Zr ratio is rather constant in each sample, around 100. Clinopyroxenes in the Japan arcs peridotite xenoliths are intermediate for Ce and Sr contents, and $(Ce/Yb)_N$ and Ti/Zr ratios. Furthermore, the most fertile peridotites from Japan arcs are similar for the clinopyroxene chemistry to the most fertile abyssal peridotites. The peridotite xenoliths from Japan arcs had possibly evolved through different process from common source peridotite to abyssal peridotite. The Japan arc mantle peridotites had been polluted by the metasomatic agent with consistent chemical characteristics due to regional mantle wedge metasomatism.

Keywords: Clinopyroxene; Peridotite; Xenoliths; Geochemical characteristics

1. Introduction

It is necessary to understand petrological characters of mantle wedge materials for consideration not only of deep structure but also of arc magmatism. Their geochemistry has been generally estimated only from the chemistry of island arc volcanic rocks because the mantle wedge materials are rare.

Peridotite xenoliths are usually brought up by alkaline basalts of intraplate type or by kimberlites and related magmas and, therefore, represent the upper mantle beneath oceanic hotspots, continental rifts and continental cratons (e.g., Nixon, 1987). Ultramafic xenoliths from the arc were derived from the mantle wedge; those included within arc-related magmas (e.g., those from Megata volcano in the Northeastern Japan arc: Kuno, 1967; Katsui et al.,

* Corresponding author. Present address Department of Earth and Planetary Sciences, Tokyo Institute of Technology, Tokyo 152, Japan.

0031-9201/98/$19.00
PII S0031-9201(97)00136-2

1979; Tanaka and Aoki, 1981; Takahashi, 1986), especially may give us direct evidence of the petrological characteristics of the mantle wedge. Arc magmas carrying mantle xenoliths are, however, very rare on Earth. In addition to the Megata xenoliths, Ninomiya and Arai (1992) reported harzburgite fragments in gabbroic xenoliths from andesite of the Oshima-Oshima volcano, northern Japan. Richard (1986) and Vidal et al. (1989) reported partly metasomatized peridotite xenoliths in calc-alkaline andesite from Batan island, the Philippines. Lherzolite xenoliths have been reported in andesite lava from Chirinkotan volcano, Kurile islands, Russia (Tsvetkov and Avdeyko, 1982) and in basalt from Mednyy

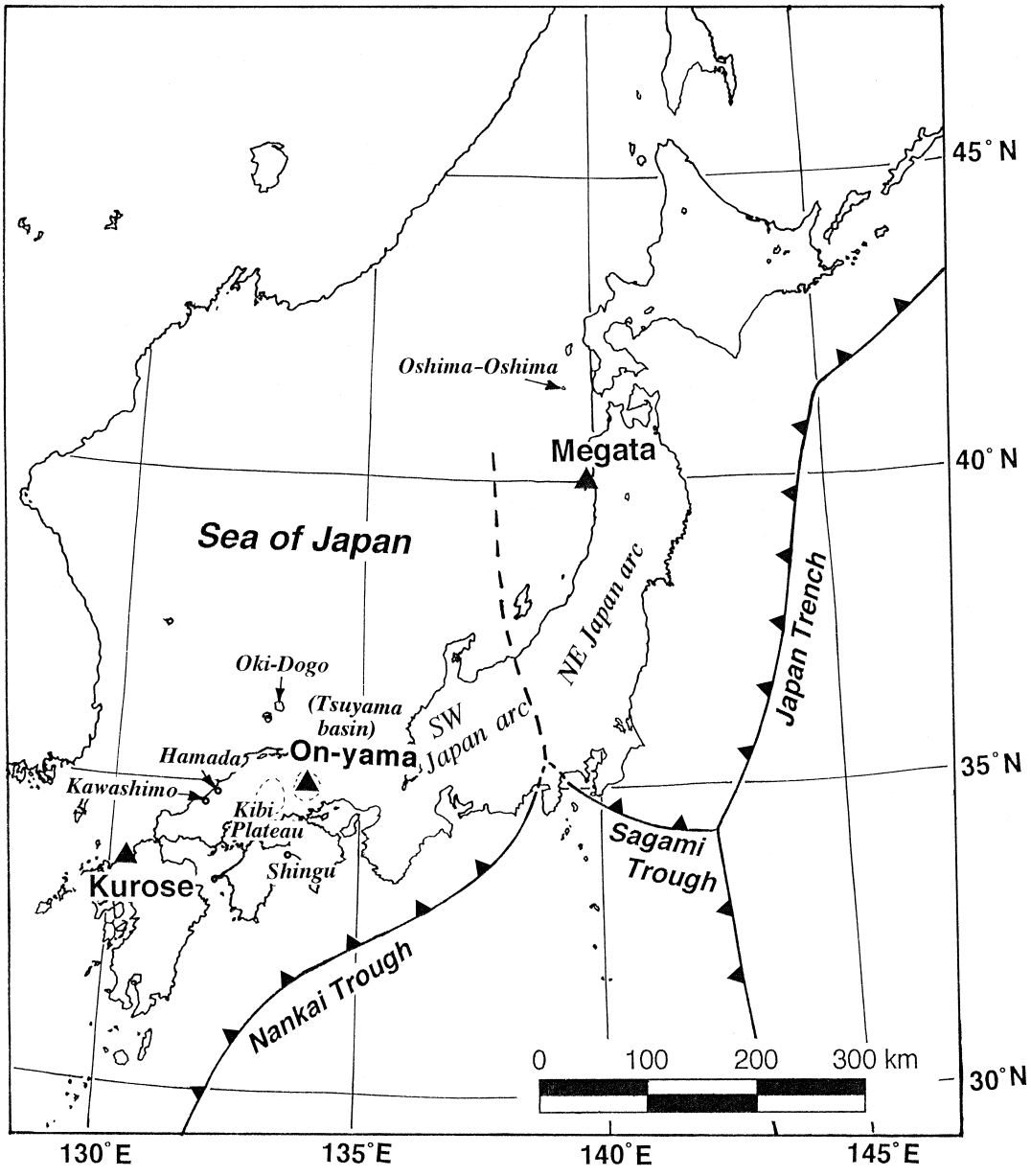

Fig. 1. Location map of the samples. For reference, other localities of residual peridotite xenoliths are shown.

Island, Komandor islands, Russia (Tsvetkov and Shmidt, 1982). Peridotite xenoliths have been found in arc magmas from the Kamchatka arc, Russia (Shcheka, 1976; Erlich et al., 1979; Shcheka, personal com. 1993).

In this paper, we would like to describe petrochemical characteristics of the peridotite xenoliths from the Japan arcs and compare them with peridotites from other tectonic settings in order to understand mantle processes beneath the arc.

As far as we know, residual peridotite xenoliths are available from nine localities on the Japan arcs (Fig. 1; Takamura, 1973; Aoki, 1987): i.e., Megata (e.g., Kuno, 1967; Abe et al., 1992; Abe and Arai, 1993) and Oshima-Oshima (Ninomiya and Arai, 1992) of the Northeast Japan arc, Kibi Plateau (Fujiwara and Arai, 1982), Tsuyama Basin (Arai and Muraoka, 1992), Oki-Dogo (Takahashi, 1978), Noyamadake (Arai and Hirai, 1983; Hirai, 1986), Kawashimo (Nagao and Sakaguchi, 1990; Arai and Abe, 1995), Kurose (Arai and Hirai, 1983; Hirai, 1986) and Shingu (Goto and Arai, 1987) of the Southwest Japan arc. Considering the degree of melt extraction, mineral composition (e.g., Arai and Muraoka, 1992; Arai, 1994) and spatial distributions of the localities (Fig. 1), we selected representative peridotite xenoliths from three localities, Megata, On-yama (Tusyama Basin) and Kurose, for detailed analyses.

2. Samples and geological setting

Thirty xenoliths of residual peridotites from three Cenozoic volcanos in the Japan arcs were examined in detail. One of the volcanos is Megata volcano from the Northeastern Japan arc, and the others are On-yama and Kurose from the Southwestern Japan arc. These three xenolithic suites have different petrographical and geographical characteristics and may represent, to some extent, the mantle materials beneath the Japan arcs. These peridotites may represent the nature of the mantle portion of the lithosphere beneath the Japan arcs. Modal compositions of the samples are shown in Table 1 and modal amount of olivine and pyroxenes for the samples are shown in Fig. 3.

Table 1
Modal compositions of peridotite xenoliths from Japan arcs

	Ol	Opx	Cpx	Sp	Amph	Mica	Symp	Others
Megata								
I-610	51.2	26.9	1.2	0.4	20.0	0.1	0.5	–
I-014	51.1	32.4	0.8	0.9	14.1	–	–	0.2
I-701	70.7	18.7	8.7	0.8	1.1	–	–	–
I-702	70.5	12.4	3.7	2.0	6.3	–	5.0	–
I-708	73.9	18.9	5.9	2.1	tr.	–	–	–
I-729	56.6	24.3	9.8	1.0	0.6	–	7.7	–
I-738-1	60.7	23.7	7.3	1.1	5	–	2.1	0.3
N-01	67.8	19.4	6.4	1.6	2.4	–	1.1	1.3
N-03	63.0	23.4	4.2	0.7	4.1	–	0.6	3.9
N-04	79.9	13.8	5.3	0.6	–	–	–	0.4
N-06	70.3	27.5	1.0	1.2	–	–	–	–
N-09	65.5	31.3	2.7	0.5	–	–	–	0.1
N-11	54.2	30.1	7.8	1.4	0.5	–	2.3	3.6
S-101	69.1	17.1	3.6	1.1	–	–	2.1	7.0
S-1001	49.1	30.9	5.7	0.9	–	–	3.6	10
S-1007	62.5	20.5	5.6	0.7	–	–	0.2	10.5
S-1019	55.6	23.2	3.4	0.6	–	–	1.3	15.9
S-111	65.6	19.4	4.8	1.5	–	–	0.1	8.6
S-469	61.4	17.0	3.8	1.8	–	–	–	16.0
Kurose								
KR-50	80.8	16.7	2.0	0.5	–	–	–	–
KR-350	78.9	18.4	2.2	0.5	–	–	–	–
KR-379	83.1	15.6	0.5	0.8	–	–	–	–
KR-392	84.4	14.1	1.4	0.1	–	–	–	–
On-yama								
ON-104	62.5	16.4	5.5	2.7	–	–	–	12.9
ON-105	69.3	15.2	3.1	1.2	–	–	–	11.2
ON-108	64.0	11.9	5.7	0.8	–	–	–	17.7
ON-110	64.7	23.2	2.4	0.7	–	–	–	8.9
ON-127	69.1	24.3	3.8	1.0	–	–	–	1.8
ON-129	66.6	23.5	3.6	1.4	–	–	–	4.9
ON-133	71.0	16.0	3.6	3.2	–	–	–	6.2

Ol, olivine; Opx, orthopyroxene; Cpx, clinopyroxene; Sp, chromian spinel; Amph, amphibole; Mica, phlogopite; Symp, pyroxene–spinel symplectite; Others are breakdown product after pargasite and 'fine-grained aggregate' surrounding pyroxene–spinel symplectite and/or reaction products between orthopyroxene and magma. I-, the sample from Ichinomegata; N-, from Ninomegata; S-, from Sannomegata; KR-, from Kurose; ON-, from On-yama.

Megata volcano located at the Oga Peninsula, the Northeast Japan arc (Fig. 1), is very famous for the abundant deep-seated xenoliths. Petrological and geochemical studies on the xenoliths have been published by many authors (e.g., Kuno, 1967; Aoki, 1971; Aoki and Prinz, 1974; Takahashi, 1980, 1986; Tanaka and Aoki, 1981). More recently Abe et al.

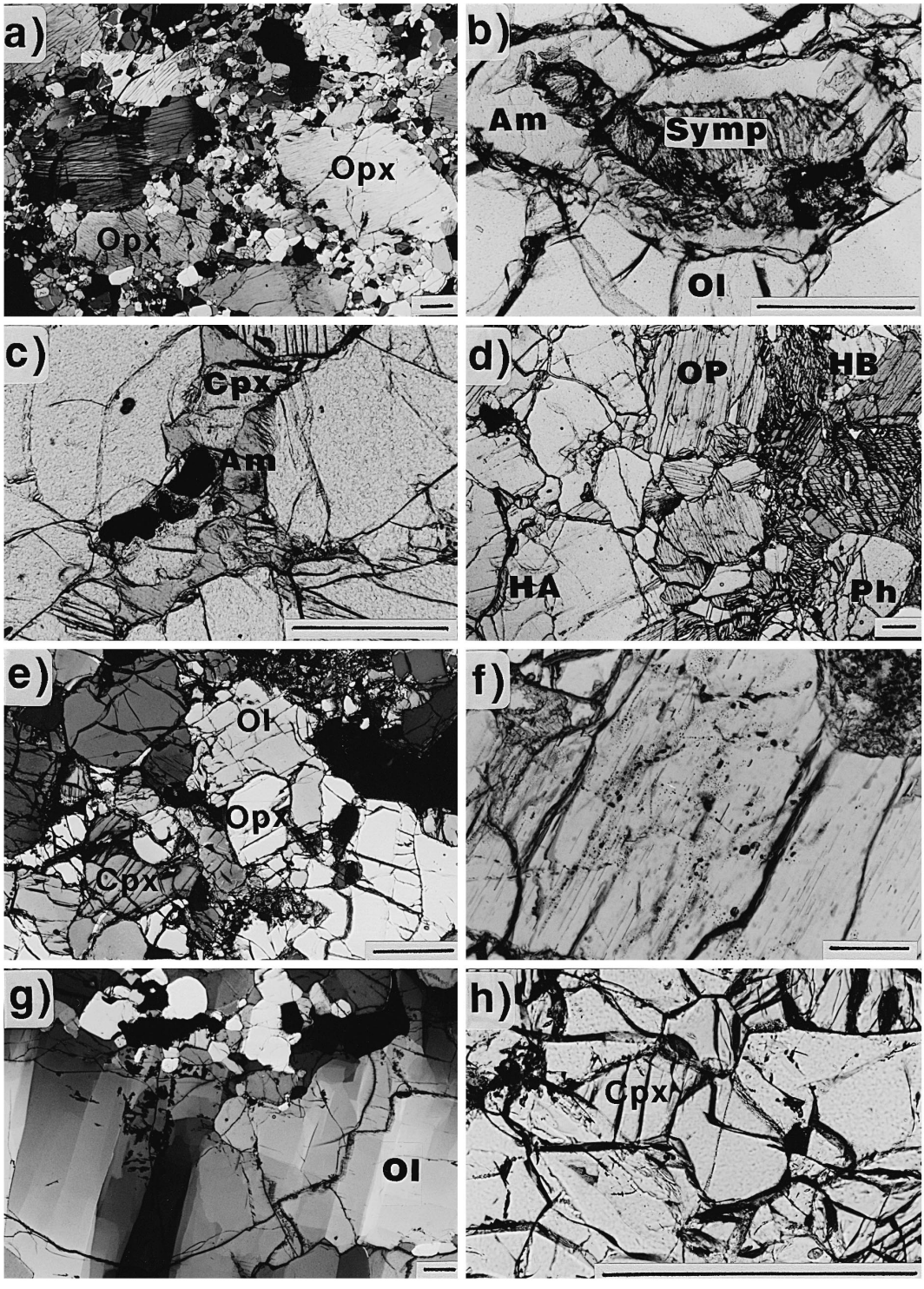
a)
Opx
Opx
b)
Am
Symp
Ol
c)
Cpx
Am
d)
OP
HB
HA
Ph
e)
Ol
Opx
Cpx
f)
g)
Ol
h)
Cpx

(1992, 1995) and Abe and Arai (1993) reported detailed petrological characteristics of the Megata peridotite xenoliths. The host magma is calc-alkali andesite to dacite, ca. 10,000 yr in age (Horie, 1964), for the Ichinomegata and Ninomegata craters, and high-alumina basalt for the Sannomegata crater (Katsui et al., 1979; Aoki and Fujimaki, 1982). Recent stratigraphical and chronological (A_c age) studies indicate that the Ichinomegata and Sannomegata craters formed from 80,000 to 60,000 yr ago and from 24,000 to 20,000 yr ago (Kitamura, 1990). In any case the activity of Megata volcano was surely in Holocene. It is noticeable that Megata volcano is one of the few places on earth where deep-seated xenoliths which have been captured by calc-alkaline magmas are available (cf. Abe and Arai, 1993).

The Megata xenolith suite is composed of peridotites, websterites, clinopyroxenites, gabbros, amphibolites, and other shallow-seated rocks (granitic and metavolcanics rocks, and sediments). Ultramafic xenoliths from Megata volcano are up to 30 cm, but usually less than 10 cm, in diameter. The peridotite xenoliths are most frequently lherzolite and less frequently harzburgite. The texture is equigranular to porphyroclastic (Fig. 2a). All ultramafic xenoliths from Megata volcano belong to Group I in the sense used by Frey and Prinz (1978). Lherzolites often have plagioclase which has reacted with olivine to various extent, producing a spinel-pyroxene symplectite (Takahashi, 1986). Peridotite, especially lherzolite, xenoliths from Ichinomegata crater have secondary pargasite (Fig. 2b and c) and rarely phlogopite, which are less than a few volume percent on average and up to 20 vol.% (e.g., Abe and Arai, 1993). The peridotites are sometimes veined by hornblendite with phlogopite (Fig. 2d). The amphiboles, mostly pargasite or pargasitic hornblende, usually replace subsolidus reaction products, such as spinel-pyroxene symplectite and exsolution lamella of clinopyroxene in orthopyroxene. Therefore, those amphiboles are mantle metasomatic minerals, due to addition of hydrous melt/fluid to dry peridotite (Abe et al., 1992; Abe and Arai, 1993).

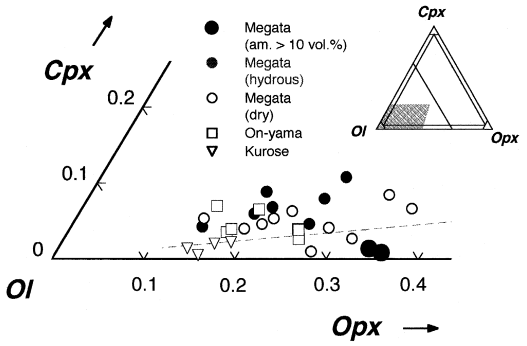

Fig. 3. Modal amounts of olivine and pyroxenes in the samples. Ol, olivine; Opx, orthopyroxene; Cpx, clinopyroxene; am., amphibole; hydrous, hydrous peridotite with amphibole; dry, dry peridotite without amphibole. The broken line shows Cpx/(Cpx + Opx) = 0.1.

On-yama is one of small monogenetic volcanos which are clustered in and around the Tsuyama Basin, southwest Japan (Fig. 1). There are no data available for the age of On-yama volcanism. However, the ages of other volcanos around On-yama in Tsuyama basin are 4.7–6.5 Ma by K–Ar method (Uto et al., 1986). Both alkali basaltic breccia and lavas of On-yama have abundant ultramafic xenoliths, which are small in size (< 5 cm across). The texture is equigranular to slightly porphyroclastic (Fig. 2e). The pyroxenes often have spinel or other inclusions (Fig. 2f). Detailed petrological data are shown in Arai and Muraoka (1992). Lherzolite is predominant among the xenoliths. Small amounts of

Fig. 2. Photomicrographs; all scale bar are 0.5 mm. Opx, orthopyroxene; Cpx, clinopyroxene; Am, amphibole; Symp, pyroxene–spinel symplectite; Ol, olivine; Ph, phlogopite; HB, hornblendite; OP, orthopyroxenite; HA, harzburgite. (a) Harzburgite from Ninomegata (N-06) with porphyroclastic texture. With cross-polarized light. (b) Lherzolite from Ichinomegata with secondary amphibole around pyroxene–spinel symplectite (I-738-1). With plane-polarized light. (c) Lherzolite from Ichinomegata with secondary amphibole around clinopyroxene (I-756, no chemical data in this paper). With plane-polarized light. (d) Harzburgite veined by hornblendite with inter-veining orthopyroxenite (I-706). With plane-polarized light. (e) Lherzolite from On-yama with equigranular (ON-133). With crossed-polarized light. (f) Spinel and other inclusions in orthopyroxene in On-yama lherzolite (ON-104). With plane-polarized light. (g) Harzburgite from Kurose with porphyroclastic texture (KR-379). With cross-polarized light. (h) Clinopyroxene in Kurose peridotite is very small (KR-392). With plane-polarized light.

other xenoliths of both Group I (wehrlite and pyroxenites) and Group II (clinopyroxenite), in the sense used by Frey and Prinz (1978) and megacrysts (clinopyroxene, spinel and phlogopite) are associated with the lherzolite. Absence of dunite is characteristic of the On-yama xenolith suite.

Kurose, located at the Hakata Bay, Fukuoka Prefecture, is composed of several small rocks of alkali basalt (Fig. 1). Uto et al. (1993) shows that the K–Ar ages for two blocks of alkali basalts from Kurose are 1.14 ± 0.12 and 1.10 ± 0.22 Ma. The activity of the Kurose is younger than other volcanics which have ultramafic xenoliths from Southwestern Japan arc. Mode of occurrence and frequency of rock species of the xenoliths, some of which are larger than 30 cm across, were briefly described by Arai and Kobayashi (1981) and Arai and Hirai (1983). The texture is porphyroclastic (Fig. 2g) and the clinopyroxene grain is very small compared with olivine or orthopyroxene porphyroclast (Fig. 2g and h). Harzburgite and clinopyroxene-poor lherzolite are dominant among the Kurose peridotite (Fig. 3; Arai and Hirai, 1983). The xenoliths derived from the so-called cumulus mantle (Takahashi, 1978) are much less abundant (less than one twentieth in volume) than those of the mantle peridotites, possibly implying the very thin cumulus mantle (Arai and Hirai, 1983). The Kurose xenolith suite is almost

Table 2
Major elements in clinopyroxene and amphibole

	I-610	I-014	I-701	I-702	I-708	I-729	I-738-1	N-01	N-03	N-11	N-04	N-06	N-09	S101	S1001	S1007
SiO_2	53.80	51.58	52.28	51.63	52.67	51.21	51.53	51.58	52.23	51.49	53.60	53.46	53.77	51.64	51.73	51.96
TiO_2	0.06	0.46	0.36	0.46	0.07	0.59	0.40	0.39	0.44	0.49	0.13	0.08	0.09	0.37	0.47	0.39
Al_2O_3	2.19	5.29	3.59	4.99	3.05	5.15	4.33	4.92	3.53	4.52	1.93	1.64	1.73	4.80	4.87	4.48
Cr_2O_3	0.56	0.98	0.64	1.14	1.18	1.16	0.92	1.16	0.77	1.12	0.80	0.56	0.57	1.18	0.93	1.15
FeO*	2.45	2.75	2.98	2.62	2.64	2.43	2.77	2.66	2.76	2.74	2.38	2.03	2.00	2.81	2.78	2.82
MnO	0.06	0.12	0.06	0.14	0.17	0.13	0.14	0.11	0.08	0.04	0.06	0.08	0.00	0.05	0.11	0.16
MgO	17.92	15.49	16.84	15.42	16.78	15.49	16.14	15.57	16.19	15.54	17.12	17.13	17.82	15.57	15.55	15.87
CaO	22.12	22.22	21.96	22.17	22.51	22.63	22.87	22.31	23.29	23.37	23.65	23.90	23.76	22.56	22.80	22.44
Na_2O	0.33	0.26	0.40	0.61	0.06	0.26	0.00	0.50	0.00	0.00	0.00	0.13	0.00	0.28	0.00	0.00
K_2O	0.00	0.03	0.00	0.03	0.00	0.02	0.00	0.01	0.00	0.00	0.00	0.00	0.00	0.07	0.00	0.01
NiO	0.00	0.26	0.15	0.21	0.20	0.21	0.11	0.22	0.00	0.16	0.14	0.20	0.18	0.08	0.21	0.17
Total	99.49	99.44	99.45	99.46	99.43	99.43	99.46	99.45	99.28	99.47	99.80	99.20	99.92	99.43	99.45	99.45
Mg#	0.929	0.910	0.910	0.913	0.919	0.919	0.912	0.912	0.913	0.910	0.928	0.938	0.941	0.908	0.914	0.909
Cr#	0.222	0.250	0.323	0.164	0.341	0.218	0.188	0.189	0.174	0.155	0.345	0.455	0.447	0.176	0.205	0.187

	S111	S469	KR50	KR350	KR379	KR392	ON104	ON105	ON108	ON110	ON127	ON129	ON133	I-610A	I-014A
SiO_2	52.47	50.99	53.14	53.02	53.56	52.70	52.10	51.73	52.88	51.62	50.88	52.29	52.20	43.80	44.44
TiO_2	0.26	0.53	0.03	0.18	0.09	0.15	0.39	0.30	0.18	0.32	0.38	0.32	0.33	0.85	0.79
Al_2O_3	2.83	4.89	3.29	3.86	2.61	3.06	3.85	3.89	4.11	4.66	5.41	4.33	4.77	14.67	12.63
Cr_2O_3	0.70	1.04	0.76	0.96	1.01	0.69	0.46	0.40	0.47	0.64	0.68	0.34	0.56	0.15	1.09
FeO*	2.74	2.98	2.69	2.71	2.47	2.65	2.95	2.87	2.76	3.08	3.63	3.04	2.78	6.89	6.79
MnO	0.09	0.04	0.04	0.22	0.13	0.09	0.12	0.16	0.11	0.06	0.14	0.10	0.09	0.21	0.12
MgO	16.42	15.87	17.26	16.54	17.18	17.20	16.86	17.01	17.11	17.09	16.66	16.52	16.76	16.48	16.55
CaO	23.48	22.70	21.43	21.65	21.65	22.22	21.60	22.09	22.06	21.89	21.49	22.51	22.07	11.50	11.49
Na_2O	0.00	0.00	0.72	0.06	0.27	0.30	0.75	0.70	0.00	0.00	0.00	0.20	0.00	2.17	2.25
K_2O	0.00	0.01	0.00	0.07	0.05	0.05	0.05	0.03	0.00	0.00	0.02	0.00	0.04	0.65	0.78
NiO	0.19	0.08	0.09	0.18	0.27	0.15	0.32	0.19	0.13	0.00	0.27	0.05	0.35	0.10	0.22
Total	99.50	99.46	99.45	99.46	99.43	99.44	99.44	99.36	99.82	99.36	99.56	99.69	99.95	97.47	97.15
Mg#	0.914	0.905	0.920	0.916	0.925	0.920	0.911	0.913	0.917	0.908	0.891	0.906	0.915	0.810	0.813
Cr#	0.160	0.203	0.372	0.299	0.474	0.304	0.148	0.146	0.157	0.149	0.118	0.151	0.131		

FeO*, total iron as FeO; Mg#, Mg/(Mg + Fe*) atomic ratio (Fe*, total Fe); Cr#, Cr/(Cr + Al) atomic ratio of chromian spinel in the sample.
I-610A and I-014A are amphibole (pargasite) and others are clinopyroxene.

free of Group II xenoliths and megacrysts (Arai and Kobayashi, 1981).

3. Mineral chemistry

3.1. Major elements

The major-element mineral compositions were measured by SEM (Akashi alpha-30) with an energy dispersive spectrometer, at Kanazawa University. Selected data for clinopyroxene and amphibole and Cr# (= Cr/(Cr + Al) atomic ratio) of chromian spinels in each samples are shown in Table 2. Cr# of spinel and Fo content of olivine in the samples which were analyzed for clinopyroxenes are shown in Fig. 4. Relations between the Cr# of spinel and modal amount and Mg/(Mg + Fe∗) ratio (= Mg#; Fe∗ means total iron) of clinopyroxene are shown in Fig. 10a and b.

Many samples of clinopyroxene in the Megata peridotites have a constant Mg# about 0.91 (Table 2); some of them have higher Mg#'s (> 0.94; Abe et al., 1992). It is noteworthy that the clinopyroxene in strongly hydrated peridotites (I-610 and I-014) also has high Mg# (Table 2). All clinopyroxenes are characteristically poor in Na_2O (Arai, 1991). Chemical data for other minerals were described and listed by Abe et al. (1992, 1995). According to Abe et al. (1992, 1995), olivine in anhydrous or slightly hydrated peridotites is Fo_{88-91} in composition. Strongly hydrated peridotites have much more Fe-enriched (down to Fo_{83}) olivine. Chromian spinel in the Ichinomegata peridotites is strongly variable in composition; Cr# varies from 0.07 to 0.53 (Table 2; Fig. 4; Abe et al., 1992, 1995). Pyroxene-spinel symplectite and plagioclase are contained only in fertile peridotites, with spinel of Cr# < 0.25. As pointed out by Abe et al. (1992), $Fe^{3+}/(Cr + Al + Fe^{3+})$ of spinel is distinctly higher in amphibole-rich peridotites than in nearly anhydrous ones. In a particular harzburgite xenolith with hornblendite selvage, the Cr# of spinel decreases towards the selvage (Abe et al., 1992).

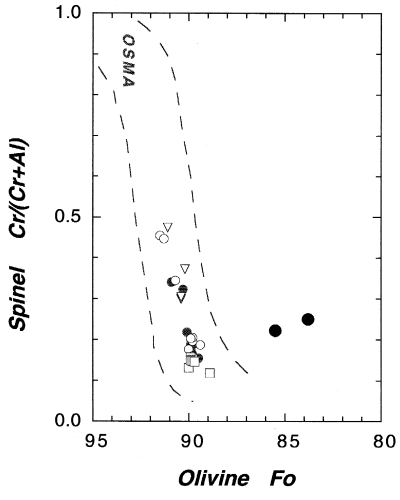

Fig. 4. Relationships between the Fo content of olivine and the Cr/(Cr + Al) atomic ratio (= Cr#) of chromian spinel in the samples. OSMA, olivine–spinel mantle array, which was proposed by Arai (1987, 1994) as a mantle peridotite restite trend formed in the spinel lherzolite field in terms of Fo content of olivine and Cr# of spinel. Symbols as in Fig. 3.

Pargasite is generally low in TiO_2 (< 1.6 wt.%), which is distinctive from amphiboles (Ti-rich pargasite to kaersutite) in peridotites from continental rift zones and oceanic hotspots (e.g., Arai, 1986). Pargasite is slightly higher both in TiO_2 content and in K/(K + Na) ratio in harzburgite than in lherzolite. K/(K + Na) ratio is the highest in the vein-forming pargasite.

Clinopyroxene in On-yama peridotites has low Mg# (0.89–0.92; Table 2) and is also poor in Na_2O. According to Arai and Muraoka (1992), the On-yama lherzolites have a rock-by-rock uniformity in mineralogy, with olivine of Fo_{89-90} and chromian spinel of Cr# = 0.10–0.15. The On-yama lherzolites are always enriched in clinopyroxene; the Cpx/(Cpx + Opx) volume ratio is higher than 0.1. The low refractoriness of the On-yama lherzolites are apparently correlated with the low frequency of associated dunite and other cumulative ultramafic xenoliths (Arai and Muraoka, 1992). The On-yama lherzolite may be representative of the least refractory part of the upper mantle beneath the Japan arcs.

Clinopyroxene in Kurose peridotites has higher Mg# (more than 0.92; Table 2) than in the On-yama lherzolites. That is also poor in Na_2O (< 0.7 wt.%) and Cr_2O_3 and Al_2O_3 contents are < 1.0 and < 3.9 wt.%, respectively. Olivine in the Kurose peridotites is rather constant in composition, between Fo_{90} and Fo_{91}, irrespective of the modal amounts of olivine and pyroxenes. They have chromian spinel of which

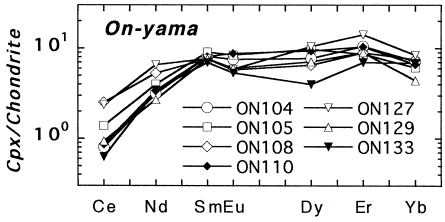

Fig. 5. Chondrite-normalized REE patterns for clinopyroxene from On-yama peridotite. All of them are depleted in light rare earth element.

Cr# is rather variable, from 0.25 to 0.55 (Table 2; Arai and Hirai, 1983).

3.2. Trace elements

Selected clinopyroxenes and amphibole were analyzed in situ for REEs and Sr, Zr and Ti using a Cameca IMS 3f ion-microprobe at Tokyo Institute of Technology. Analytical procedure was described by Yurimoto et al. (1989). The data are presented in Table 3. Relations between Cr# of coexisting spinel and Ce_N, Yb_N, Sr_N, $(Ce/Yb)_N$ ratio, Ti and Zr wt.% and Ti/Zr weight ratio of clinopyroxenes are shown in Fig. 10c–i. Their REE patterns are shown in Figs. 5–9 (Chondrite normalizing values from Anders and Ebihara, 1982).

As with the case of the major elements, On-yama samples are relatively homogeneous with respect to contents of Ti, Zr and Sr (Table 3) and their chondrite-normalized REE patterns (Fig. 5). Ti and Zr are relatively abundant; 1003 to 1400 and 3.9 to 10.3 ppm (Table 3), respectively. However, Sr contents are low (Table 3), 3.5 to 12.1 ppm. Chondrite-normalized REE patterns are LREE-depleted convex-upward (Fig. 5). Their $(Ce/Yb)_N$ and Ti/Zr ratio

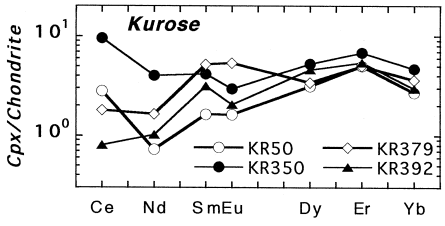

Fig. 6. Chondrite-normalized REE patterns for clinopyroxene from Kurose peridotite. They are depleted in heavy rare earth element.

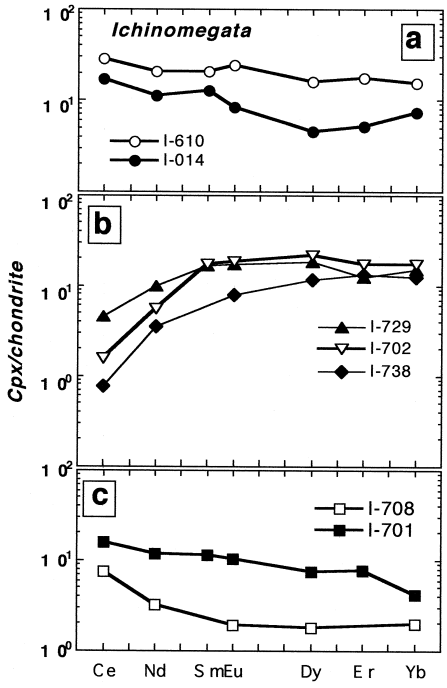

Fig. 7. Chondrite-normalized REE patterns for clinopyroxene from Ichinomegata peridotite. (a) For strongly hydrated peridotite. (b) For lherzolite with pyroxene–spinel symplectite. (c) For lherzolite without pyroxene–spinel symplectite. All of the samples from Ichinomegata, analyzed in this paper, include small amount or abundant amount of amphibole.

are comparatively constant, 0.1 to 0.3 and 106 to 260, respectively.

Samples from Kurose are even less variable in Ti, Zr and Sr abundances (273 to 546, 0.9 to 3.0 and 4.8

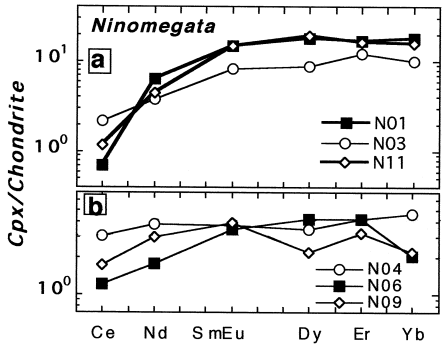

Fig. 8. Chondrite-normalized REE patterns for clinopyroxene from Ninomegata peridotite. (a) For hydrous lherzolite with symplectite. (b) For dry lherzolite and harzburgite without amphibole.

Table 3
Rare earth elements, Ti, Zr and Sr abundances in clinopyroxene and amphibole

	I-610	I-014	I-701	I-702	I-708	I-729	I-738-1	N-01	N-03	N-04	N-06	N-09	N-11	S-101	S-1001	S-1007	S-1019
Ti	3215	965	1354	2512	206	3057	2757	3304	2313	728	367	454	3620	3142	3114	3140	2985
Zr	30.1	12.2	15.1	14.1	1.6	29.4	10.8	11.2	17.4	6.5	3.6	4.1	14.0	10.0	15.4	23.3	12.9
Sr	86.4	41.3	52.0	2.9	7.0	6.8	6.3	0.9	9.1	19.8	11.5	13.1	1.8	1.3	6.8	7.1	6.7
Ce	17.56	10.37	9.72	0.96	4.62	2.79	0.47	0.43	1.36	1.89	0.75	1.08	0.74	0.50	0.66	1.54	1.00
Nd	9.46	5.10	5.36	2.48	1.45	4.49	1.59	2.91	1.73	1.73	0.81	1.38	2.05	1.54	1.96	4.09	2.97
Sm	3.01	1.90	1.71	2.58	–	2.50	–	–	–	–	–	–	–	–	–	–	–
Eu	1.33	0.47	0.57	1.03	0.11	0.95	0.44	0.83	0.45	0.21	0.19	0.22	0.83	0.62	0.69	0.78	0.67
Dy	3.81	1.11	1.79	5.25	0.43	4.41	2.86	4.42	2.14	0.85	1.03	0.55	4.68	4.26	4.44	4.92	4.57
Er	2.77	0.81	1.22	2.73	0.61	1.95	2.15	2.69	1.92	0.67	0.66	0.52	2.58	3.40	2.32	2.79	3.32
Yb	2.42-	1.16	0.66	2.70	0.31	2.40	1.97	2.86	1.59	0.73	0.33	0.35	2.50	2.18	3.09	2.46	2.94

	S-111	S-469	K-R50	KR-350	KR-379	KR-392	ON-104	ON-105	ON-108	ON-110	ON-127	ON-129	ON-133	I-610A	I-014A
Ti	1320	1736	173	546	273	422	1038	1274	1097	1107	1399	1003	1167	4712	3680
Zr	4.9	6.5	0.9	3.0	1.6	0.9	5.5	6.9	10.3	5.6	9.4	3.9	5.0	56.5	51.0
Sr	5.2	14.7	8.2	52.4	12.6	4.8	3.5	7.2	12.1	4.1	11.3	8.5	5.5	180.8	178.5
Ce	1.48	4.58	1.73	5.90	1.11	0.50	0.50	0.86	1.56	0.53	1.46	0.58	0.39	20.28	16.00
Nd	1.01	1.78	0.33	1.83	0.75	0.47	1.44	1.83	2.42	1.55	3.00	1.24	1.58	11.17	14.64
Sm	–	–	0.24	0.62	0.77	0.47	1.21	1.35	1.14	1.20	1.15	1.13	1.04	3.43	3.69
Eu	0.29	0.46	0.09	0.17	0.30	0.11	0.42	0.47	0.32	0.49	0.33	0.34	0.30	1.70	0.49
Dy	1.03	1.49	0.77	1.29	0.83	1.12	1.89	2.38	1.60	2.30	2.57	1.74	0.98	3.56	1.79
Er	0.88	1.33	0.80	1.09	0.80	0.87	1.68	1.38	1.43	1.66	2.25	1.44	1.12	–	–
Yb	1.14	1.24	0.43	0.74	0.57	0.47	1.14	0.97	1.20	1.06	1.34	0.70	1.09	2.22	1.18

I-610A and I-014A are amphibole (pargasite) and others are clinopyroxene.

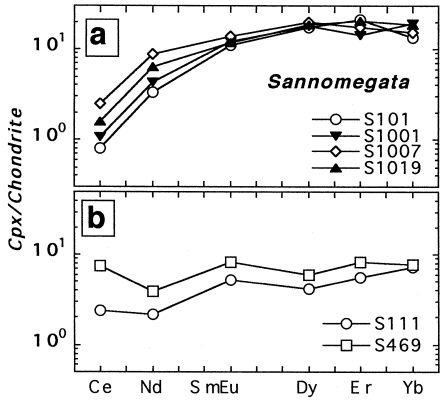

Fig. 9. Chondrite-normalized REE patterns for clinopyroxene from Sannomegata peridotite. (a) For lherzolite with abundant pyroxene–spinel symplectite. (b) For lherzolite with porphyroclastic texture. One of them has small amount of pyroxene–spinel symplectite and the other has none.

to 52.5 ppm, respectively) (Table 3). However, chondrite-normalized REE patterns are variable from flat to slightly LREE-depleted, being very depleted in all REEs (Fig. 6). Their Ti/Zr ratio is constant; 166–467, but $(Ce/Yb)_N$ varies from 0.2 to 2.0.

In contrast to the On-yama and Kurose cases, the samples from Megata volcano are variable for both trace elements abundance (Table 3) and chondrite-normalized REE patterns (Figs. 7–9). The Ti, Zr and Sr contents are 200 to 3620, 1.6 to 30.1 and 0.9 to 86.4 ppm, respectively. The most hydrated peridotite (Table 3; I-610) has clinopyroxene which is most enriched in Ti, Zr, Sr and Ce, and its chondrite-normalized REE pattern is LREE-enriched. The $(Ce/Yb)_N$ varies greatly from 0.04 to 4.0 and the Ti/Zr ratio varies from 90 to 313 ppm but the majority contain about 100 ppm.

4. Discussion

4.1. Comparisons with the peridotites from other tectonic settings

The modal amounts of minerals and major-element chemistry of the minerals indicate that the samples in this paper are typical of the peridotite xenoliths from the Japan arcs. Their Cpx/(Cpx + Opx) volume ratios vary from less than 0.1 to more than 0.3 (Fig. 3). The Cr#'s of spinel vary widely from 0.1 to 0.5; they cover the range of the peridotite xenoliths from the Japan arcs (Table 2; Fig. 4), which are representative of residual peridotites with various degrees of melt extraction. Furthermore, they are suitable for consideration of arc mantle metasomatism, because they are composed of both hydrous and anhydrous peridotites (Abe et al., 1992); some of them have been modified by 'modal metasomatism' and possibly by 'cryptic metasomatism' (Dawson, 1984). We have compared our analytical data with published data for abyssal peridotites (Dick, 1989; Johnson et al., 1990) and peridotite xenoliths from other settings (e.g., Menzies et al., 1985; Stosch and Lugmair, 1986; Sen et al., 1993). Most of the data are for spinel- and/or plagioclase-facies mantle peridotites, some of them are for garnet-facies. The data of the peridotite xenoliths from kimberlite are excluded. The analytical data from literature are mainly by using SIMS, and instrumental and radiochemical neutron activation and isotope dilution techniques for some samples.

In Fig. 10 relations between Cr# of spinel and chemistry of clinopyroxene are shown for the peridotites from the Japan arcs and from the ocean floor (Dick, 1989; Johnson et al., 1990). It is believed that Cr# of spinel increases with an increase of degree of melt extraction in the mantle peridotite. If the peridotites were products of simple melt extraction, incompatible elements have to decrease with an increase of Cr# of spinel. Ce, Yb, Ti, Zr and Sr contents of examined clinopyroxene from Japan arcs have, however, no clear correlations with Cr# of spinel (Fig. 10). Ce content does not decrease with an increase of Cr# of spinel (Fig. 10d). $(Ce/Yb)_N$ ratio slightly increases rather than decreases with an increase of Cr# of spinel (Fig. 10e). Such a correlation between REE and major element contents in mantle peridotites was first recognized in the peridotite xenoliths by Frey and Green (1974), and has been reported from many peridotite xenoliths and massif peridotites all over the world except for the abyssal peridotites (cf. Frey, 1984; McDonough and Frey, 1989). Furthermore, Ti/Zr ratio is constant or slightly decreases with an increase of Cr# of spinel (Fig. 10i). The peridotites from Japan arcs have slightly less volume of clinopyroxene than that of abyssal peridotites (Fig. 10a). In terms of their ma-

jor-element chemistry of minerals (cf. Arai, 1994) and trace-element contents of clinopyroxene, however, the fertile sample from Japan arcs is quite similar to the fertile one of abyssal peridotite. It is possible, therefore, that the peridotites from Japan arcs had shared the same source with the abyssal

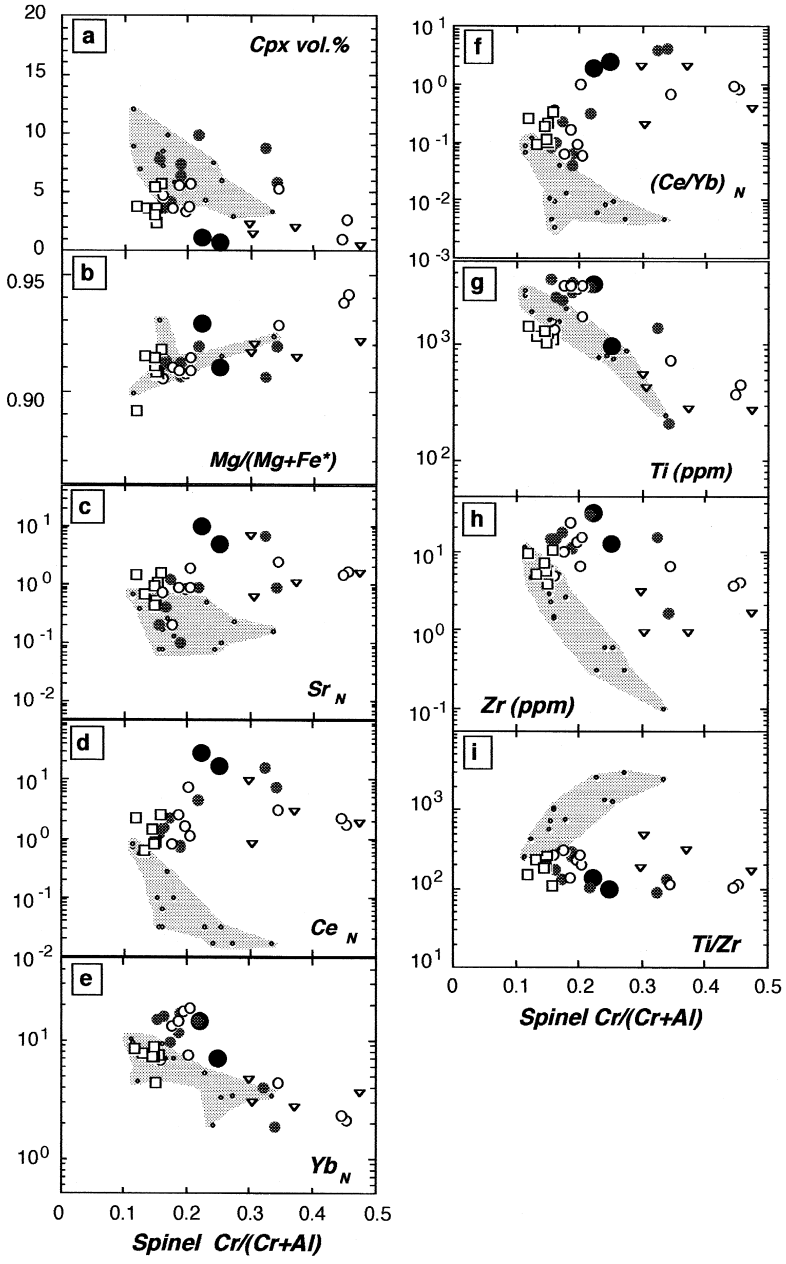

Fig. 10. Relations between the Cr# of spinel and other characteristics of clinopyroxenes. (a) Modal amount. (b) Mg/(Mg + Fe∗) ratio (= Mg#; Fe∗ means total iron). (c) Sr_N. (d) Ce_N. (e) Yb_N. (f) $(Ce/Yb)_N$ ratio. (g) Ti concentration (ppm). (h) Zr concentration (ppm). (i) Ti/Zr weight ratio. For comparison, ranges for abyssal peridotites (shaded) (Dick, 1989; Johnson et al., 1990) are shown. Symbols as in Fig. 3.

peridotite, but they had evolved through different processes.

For comparison with peridotite xenoliths from other settings, the modal amount of clinopyroxene in the samples vs. Ce, Yb, Ti, Zr and Sr contents, and $(Ce/Yb)_N$ and Ti/Zr ratios in the clinopyroxene are shown in Fig. 11.

If the peridotites had evolved through simple melt extraction from pyrolite without pollution of exotic melt/fluid, their clinopyroxenes show similar trends in terms of trace-element contents to that of the abyssal peridotites, which are simple residue (Johnson et al., 1990). Clinopyroxenes in both peridotite xenoliths from the Japan arcs and other settings, however, do not show the trends by abyssal peridotite in terms of trace elements except Yb_N and Ti.

It is noteworthy that the clinopyroxenes from Japan arc mantle peridotites are obviously distinguished from those of abyssal peridotites and the peridotite xenoliths from other tectonic settings for Ce and Sr contents and $(Ce/Yb)_N$ and Ti/Zr ratios. Arai (1991) demonstrated a similar relation; Na_2O

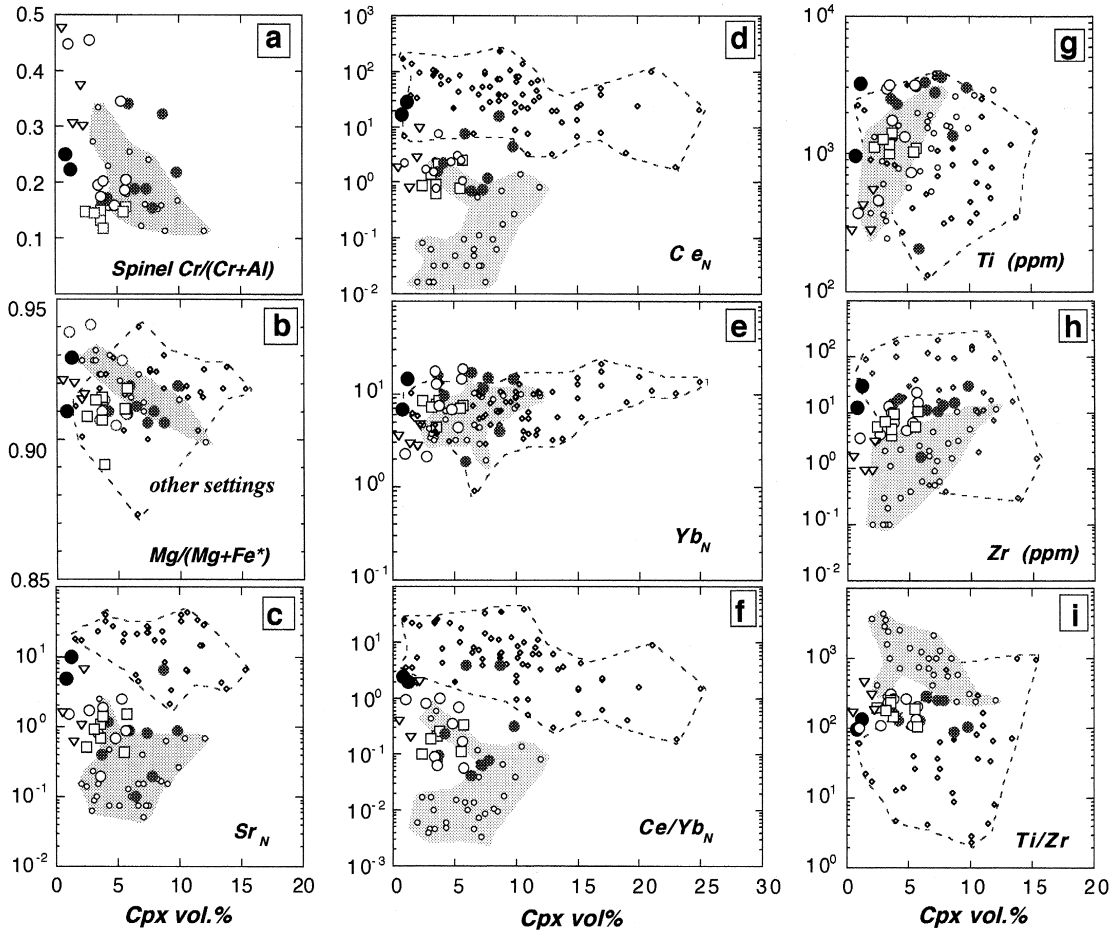

Fig. 11. Relationships between clinopyroxene modal amount and (a) Cr# of spinel, (b) Mg/(Mg + Fe*) atomic ratio, (c) Sr_N, (d) Ce_N, (e) Yb_N, (f) $(Ce/Yb)_N$ ratio, (g) Ti concentration (ppm), (h) Zr concentration (ppm) and (i) Ti/Zr weight ratio for clinopyroxene in the Japan arc peridotites (larger symbols). For comparison, ranges for abyssal peridotites (shaded) and peridotite xenoliths from other settings (enclosed by the broken line) are shown. Data of other settings are after Frey and Prinz (1978), Menzies et al. (1985), Salters and Shimizu (1988), Sen et al. (1993), Stosch and Lugmair (1986), Witt-Eickshen et al. (1993), Alibert (1994) and Blusztajn and Shimizu (1994). Symbols as in Fig. 3.

content in clinopyroxene from Japan arc mantle is intermediate between abyssal peridotites (low) and oceanic hotspot and continental rift peridotites (high). It is especially interesting that the Ti/Zr ratio is nearly constant, almost from 100 to 300 (Fig. 10i, Fig. 11i, Fig. 13).

4.2. The effect of formation of hydrous minerals

The partition coefficients (D) for REE and other trace elements between melt or fluid and solid phases are different according to the minerals concerned. D values for trace elements between hornblende (pargasite) and clinopyroxene (diopside) are not unity; the D values of pargasite/diopside for REE, Sr, Y, Zr and Hf from mantle peridotites of Eifel, Germany, vary from 1 to 8 (Witt-Eickschen and Harte, 1994). Clinopyroxene of the most hydrated sample, I-610 (Table 3), has high REE and Ti, Zr and Sr contents. The partition coefficients for these elements of hornblende/clinopyroxene pairs are low ($D = 0.9$ to 2.1). On the other hand, REE contents of clinopyroxene from a strongly hydrated sample, I-014 (Table 3), are rather low, and the D values of hornblende/clinopyroxene are higher ($D = 1.4$ to 4.3) than for the most hydrated sample (I-610). In other samples the partition coefficients for hornblende/clinopyroxene pairs vary widely without any correlations with the volume of hornblende and clinopyroxene in the samples (Abe and Yurimoto, unpublished). The difference of REE and other trace-element abundances in clinopyroxene, therefore, cannot be completely explained by the difference in degree of hydration.

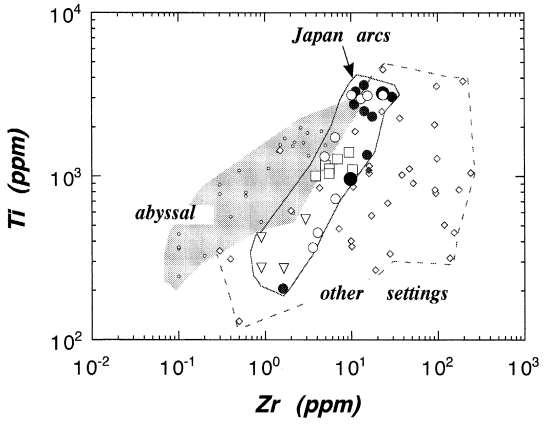

Fig. 12. Relationship between Ti and Zr concentrations (ppm) in clinopyroxene of Japan arc peridotites (larger symbols). Symbols as in Fig. 3. Note that the trend for the Japan arc peridotites is different from that of the abyssal peridotite.

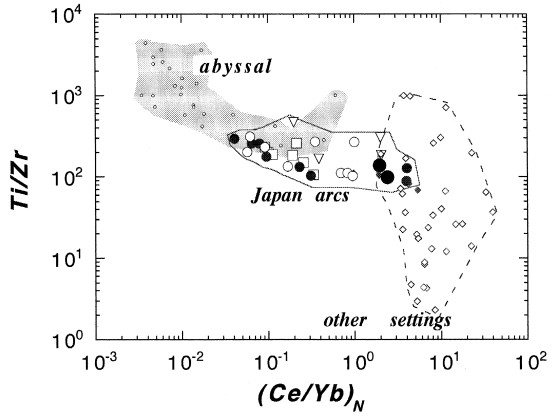

Fig. 13. Ti/Zr ratio vs. $(Ce/Yb)_N$ ratio in clinopyroxene in the peridotite. The clinopyroxene in the Japan arc peridotites is rather constant with Ti/Zr ratio of about 100 and intermediate value of $(Ce/Yb)_N$ ratio between abyssal peridotites and peridotite xenoliths from other settings. The clinopyroxene from the Japan arcs are obviously different from others. Symbols as in Fig. 3.

4.3. Geochemical characteristics of the Japan arc peridotite xenoliths

Clinopyroxenes of hydrous peridotites from Megata volcano are relatively rich in Ti to those of anhydrous peridotite from abyssal and other tectonic settings. If the metasomatizing agent which formed hydrous minerals in Megata peridotites was arc magma, it is unlikely for the clinopyroxene to have high Ti content. It is more probable that hydrous melt or fluid which was metasomatic agent added Ti to the Megata peridotite.

The residue left after partial melting should have a higher Ti/Zr ratio than the source material because Zr is more incompatible than Ti (Hart and Dunn, 1993). The Ti/Zr ratio of clinopyroxene from abyssal peridotite (Johnson et al., 1990) increases up to 4430 with an increase of melt extraction. Addition of a metasomatic component commonly leads to a decrease of the Ti/Zr ratio of clinopyroxene (Figs. 12

and 13; Blusztajn and Shimizu, 1994). Compared with the clinopyroxene in abyssal peridotites as representative of residue after partial melting, those in the peridotite xenoliths from Japan arcs are enriched in incompatible elements such as Sr, Zr and Ce. The $(Ce/Yb)_N$ ratios slightly increases and the Ti/Zr ratios is rather constant with an increase of Cr# of spinel in the Japan arc peridotites (Fig. 10f and i). The trends of these ratios in clinopyroxene cannot be due to simple melt extraction, but the peridotites are metasomatized and/or polluted by some metasomatic agent with a nearly constant Ti/Zr ratio (Fig. 13). If the metasomatic melt or fluid is percolated chromatographically once or more times into the peridotite locally, the Ti/Zr ratio may be rather variable spatially.

It appears that wedge mantle metasomatism is a regional phenomenon establishing to give the common geochemical characteristics to the sub-arc peridotites.

5. Conclusions

Clinopyroxenes in the peridotite xenoliths from three localities of the Japan arcs are geochemically distinguished from those in abyssal peridotites and peridotite xenoliths from other tectonic settings including continental rifts and oceanic hotspots. Their incompatible elements' contents are higher than those in abyssal peridotite and lower than in the peridotite xenoliths from other tectonic settings. Their Ti/Zr and $(Ce/Yb)_N$ ratios are rather constant; 90 to 313 and 0.04 to 4.0, respectively.

We conclude that the Japan arcs mantle peridotites have been polluted by a metasomatic agent with relatively consistent chemical characteristics accompanying regional mantle wedge metasomatism.

Acknowledgements

We are very grateful to Y. Saeki, H. Muraoka and H. Hirai, who approved our access to thin sections. Many people helped us to collect xenolith samples. We are much indebted to K. Hisada for his kindness and for his accommodation. We benefitted from advice of A. Ishiwatari and M. Okuno in SEM analysis. M. Kida kindly drafted some of the figures used in this paper. We are grateful to anonymous reviewers for their comments which greatly helped us in improving the former manuscript.

References

Abe, N., Arai, S., 1993. Petrographical characteristics of ultramafic xenoliths from Megata volcano, the Northeast Japan arc. Sci. Rep., Kanazawa Univ. 38, 1–24.

Abe, N., Arai, S., Saeki, Y., 1992. Hydration processes in the arc mantle; petrology of the Megata peridotite xenoliths, the Northeast Japan arc. J. Mineral. Petrol. Econ. Geol. 87, 305–317, (in Japanese, with English abstract).

Abe, N., Arai, S., Ninomiya, A., 1995. Peridotite xenoliths and essential ejecta from the Ninomegata crater, the northeastern Japan arc. J. Mineral. Petrol. Econ. Geo. 90, 41–49, (in Japanese, with English abstract).

Alibert, C., 1994. Peridotite xenoliths from western Grand Canyon and the Thumb: a probe into the subcontinental mantle of the Colorado Plateau. J. Geophys. Res. 99, 21605–21620.

Anders, E., Ebihara, E., 1982. Solar-system abundances of the elements. Geochim. Cosmochim. Acta 46, 2363–2380.

Aoki, K., 1971. Petrology of mafic inclusions from Itinome-gata. Jpn. Contrib. Mineral. Petrol. 30, 314–331.

Aoki, K., 1987. Japanese island arc: xenoliths in alkali basalts, high-alumina basalts a, and calc-alkaline andesites and dacites. In: P.H. Nixon (Ed.), Mantle Xenoliths. Wiley, New York, pp. 319–333.

Aoki, K., Prinz, M., 1974. Chromian spinels in lherzolite inclusions from Itinome-gata. Jpn. Contrib. Mineral. Petrol. 18, 326–337.

Aoki, K., Fujimaki, H., 1982. Petrology and geochemistry of calc-alkalin andesite of presumedupper mantle prigin from Itinome-gata. Jpn. Am. Mineral. 67, 1–13.

Arai, S., 1986. K/Na variation in phlogopite and amphibole of upper mantle peridotites due to fractionation of the metasomatizing fluids. J. Geol. 96, 436–444.

Arai, S., 1987. An estimation of the last depleted spinel peridotite on the basis of olivine spinel mantle array. N. Jb. Miner. Mh. 1987. 347–354

Arai, S., 1991. Petrological characteristics of the upper mantle peridotites beneath the Japan island arcs—petrogenesis of spinel peridotites. Sov. Geol. Geophys. 32, 8–25.

Arai, S., 1994. Characterization of spinel peridotites by olivine–spinel compositional relationships: review and interpretation. Chem. Geol. 113, 191–204.

Arai, S., Kobayashi, Y., 1981. Frequency of ultramafic rocks as inclusions in some alkali basalts from southwestern Japan and its bearing on the constitution of the upper mantle. Ann. Rep., Inst. Geosci., Univ. Tsukuba 7, 66–69.

Arai, S., Hirai, H., 1983. Petrographical notes on deep-seated and related rocks: 1. Mantle peridotites from Kurose and Noyamadake alkali basalts, southwestern Japan. Ann. Rep., Inst. Geosci., Univ. Tsukuba 9, 65–67.

Arai, S., Muraoka, H., 1992. Peridotite xenoliths in alkali basalts from On-yama, the Chugoku district, as a suite of fertile upper mantle peridotites beneath the southwest Japan arc. J. Mineral. Petrol. Econ. Geol. 87, 240–251, (in Japanese, with English abstract).

Arai, S., Abe, N., 1995. Reaction of orthopyroxene in peridotite xenoliths with alkali-basalt melt and its implication for genesis of alpine-type chromitite. Am. Mineral. 80, 1041–1047.

Blusztajn, J., Shimizu, N., 1994. The trace-element variations in clinopyroxenes from spinel peridotite xenoliths from southwest Poland. Chem. Geol. 111, 227–243.

Dawson, J.B., 1984. Kimberlites: II. The mantle and crust/mantle relationships. In: Kornprobst, J. (Ed.), Developments in Petrology Series,.Elsevier, Amsterdam, 11B, pp. 290–294.

Dick, H.J.K., 1989. Abyssal peridotites very slow spreading ridges and ocean ridge magmatism. In: Saunders, A.D., Norry, M.J. (Eds.), Magmatism in the Ocean Basins. Geol. Soc. London, Spec. Publ., 42, pp. 597–628.

Erlich, E.N., Kutyev, F.Sh., Bogoyavlenskaya, G.E., Tolstikhin, I.N., Mamyrin, B.A., Khabarin, L.V., 1979. Cognate inclusions in basalt–andesite rock series. In: Erlich, E.N., Gorshkov, G.S. (Eds.), Quaternary Volcanism and Tectonics in Kamchatka. Bull. Vol. 42: 152–166.

Frey, F.A., 1984. Rare earth abundances in upper mantle rocks. In: Henderson, P. (Ed.), Rare Earth Element Geochemistry. Elsevier, Amsterdam, pp. 153–203.

Frey, F.A., Green, D.H., 1974. The mineralogy, geochemistry and origin of lherzolite inclusions in Victorian basanites. Geochim. Cosmochim. Acta 38, 1023–1059.

Frey, F.A., Prinz, M.A., 1978. Ultramafic inclusions from San Carlos, Arizona: petrologic and geochemical data bearing on their petrogenesis. Earth Planet. Sci. Lett. 38, 129–176.

Fujiwara, M., Arai, S., 1982. Ultramafic xenoliths in Arato-yama alkali basalt, Okayama prefecture, as upper mantle materials beneath a typical island arc. J. Jpn. Assoc. Mineral. Petrol. Econ. Geol. 64, 107–122, (in Japanese, with English abstract).

Goto, K., Arai, S., 1987. Petrology of peridotite xenoliths in lamprophyre from Shingu, southwestern Japan: implications for origin of Fe-rich mantle peridotites. Mineral. Petrol. 37, 137–155.

Hart, S.R., Dunn, T., 1993. Experimental cpx/melt partitioning of 24 elements. Contrib. Mineral. Petrol. 113, 1–8.

Hirai, H., 1986. Petrology of ultramafic xenoliths from Noyamadake and Kurose, southwestern Japan. D. Sc. thesis, Univ. of Tsukuba, Tsukuba, 181 pp.

Horie, S., 1964. Some age data for the study on development of lakes. Kagaku (Science), Iwanami 34, 98, (in Japanese).

Johnson, K.T., Dick, H.J.B., Shimizu, N., 1990. Melting in the oceanic upper mantle: ion microprobe study of diopsides in abyssal peridotites. J. Geophys. Res. 95, 2661–2678.

Katsui, Y., Yamamoto, M., Nemoto, S., Niida, K., 1979. Genesis of calc-alkalic andesites from Oshima-Oshima and Ichinomegata volcanoes. North Jpn. J. Fac. Sci. Hokkaido Univ. 19, 157–168.

Kitamura, S., 1990. Ages of Megata maars in the Oga peninsula. Jpn. Ann. Tohoku Geogr. Assoc. 42, 161–167.

Kuno, H., 1967. Mafic and ultramafic nodules from Itinome-gata Japan. In: Wylie, P.J. (Ed.), Ultramafic and Related Rocks. Wiley, New York, pp. 337–342.

McDonough, W.F., Frey, F.A., 1989. Rare earth elements in upper mantle rocks. In: Lipin, B.R., McKay, G.A. (Eds.), Geochemistry and Mineralogy of Rare Earth Elements. Mineral. Soc. Am., Washington, DC, Reviews in Mineralogy, 21, pp. 99–146.

Menzies, M., Kempton, P., Dungan, M., 1985. Interaction of continental lithosphere and asthenospheric melts below the Geronimo Volcanic Field, Arizona, USA. J. Petrol. 26, 663–693.

Nagao, T., Sakaguchi, Y., 1990. Ultramafic xenoliths in the cenozoic kawashimo alkali basalt from Masuda, Shimane prefecture, SW Japan. J. Mineral. Petrol. Econ. Geol. 85, 469–480, (in Japanese, with English abstract).

Ninomiya, A., Arai, S., 1992. Harzburgite fragment in a composite xenolith from an Oshima-Oshima andesite, the Northeast Japan arc. Bull. Volcanol. Soc. Jpn. 37, 269–273, (in Japanese).

Nixon, P.H., 1987. Mantle Xenoliths. Wiley, New York, 844 pp.

Richard, M., 1986. Géologie et Pétrologie d'un Jalon de L'arc Taiwan-Luzon: L'ile de Batan (Philippines). Thèse de Doctrat de L'Université de Bretagne Occidentale, in French with English abstract, 351 pp.

Salters, V.J.M., Shimizu, N., 1988. World-wide occurrence of HFSE-depleted mantle. Geochim. Cosmochim. Acta 52, 2177–2182.

Sen, G., Frey, F.A., Shimizu, N., Leeman, W.P., 1993. Evolution of the lithosphere beneath Oahu, Hawaii: rare earth element abundances in mantle xenoliths. Earth Planet. Sci. Lett. 119, 53–69.

Shcheka, S.A., 1976. Evidence of metamorphism of ultramafic inclusions before their incorporation into basalt magma. Dokl. Akad. Nauk. (Earth Sci.) 227, 704–707.

Stosch, H.-G., Lugmair, G.W., 1986. Trace element and Sr and Nd isotope geochemistry of peridotite xenoliths from the Eifel (West Germany) and their bearing on the evolution of the subcontinental lithosphere. Earth Planet. Sci. Lett. 80, 281–298.

Takahashi, E., 1978. Petrologic model of the crust and upper mantle of the Japanese island arcs. Bull. Volcanol. 41, 529–547.

Takahashi, E., 1980. Thermal history of lherzolite xenoliths—petrology of lherzolite xenoliths from the Ichinomegata crater, Oga Peninsula, northeast Japan, Part I. Geochim. Cosmochim. Acta. 44, 1643–1658.

Takahashi, E., 1986. Genesis of calc-alkali andesite magma in anhydrous mantle crust boundary: petrology of lherzolite xenoliths from the Ichinomegata crater, Oga peninsula, northeast Japan, part II. J. Volcanol. Geotherm. Res. 29, 355–395.

Takamura, H., 1973. Petrographical and petrochemical studies of the cenozoic basaltic rocks in Chugoku province. Geol. Rep., Hiroshima Univ. 18, 1–167, (in Japanese, with English abstract).

Tanaka, T., Aoki, K., 1981. Petrogenic implications of REE and Ba data on mafic and ultramafic inclusions from Itinome-gata. Jpn. J. Geol. 89, 369–390.

Tsvetkov, A.A., Avdeyko, G.P., 1982. First find of lherzolite inclusions in lavas erupted in 1980 from the Chirinkotan volcano, Kurile islands. Dokl. Akd. Nauk 267, 133–137.

Tsvetkov, A.A., Shmidt, O.A., 1982. First finds of plutonic inclusions in igneous rocks of the Komandor islands. Dokl. Akd. Nauk 267, 123–127.

K. Uto, H. Hirai, S. Arai, 1986. K–Ar ages of some xenolith-bearing alkali basalts rom southwestern Japan. Abst. Ann. Joint Meet. Jpn. Assoc. Petrol. Mineral. Econ. Geol., Mineral. Soc. Jpn., Soc. Min. Geo. Jpn., 115 (in Japanese).

Uto, K., Hirai, H., Arai, S., 1993. K–Ar ages for quaternary alkali basalts from Kurose, Fukuoka prefecture and Kufune, Yamaguchi prefecture Southwest Japan. Bull. Geol. Surv. Jpn. 44, 693–698, (in Japanese, with English abstract).

Vidal, P., Dupuy, C., Maury, R., Richard, M., 1989. Mantle metasomatism above subduction zones: trace-element and radiogenic isotope characteristics of peridotite xenoliths from Batan island (Philippines). Geology 17, 1115–1118.

Witt-Eickschen, G., Harte, B., 1994. Distribution of trace elements between amphibole and clinopyroxene from mantle peridotites of the Eifel (Western Germany): an ion-microprobe study. Chem. Geol. 117, 235–250.

Witt-Eickshen, G., Seck, H.A., Reys, C.H., 1993. Multiple enrichment processes and their relationships in the subcrustal lithosphere beneath the Eifel (Germany). J. Petrol. 34, 1–22.

Yurimoto, H., Yamashita, A., Nishida, N., Sueno, S., 1989. Quantitative SIMS analysis of GSJ rock reference samples. Geochem. J. 23, 215–236.